

Banff International Workshop on Induced Seismicity

24-26 October, 2018

Expanded Abstracts



Banff International Workshop on Induced Seismicity

24-26 October, 2018

Expanded Abstracts

1. Braun, T., Cesca, S., Dahm, T., Danesi, S. and Morelli, A. **Monitoring of Anthropogenic Seismicity in Italy: State of the Art**
2. Eaton, D.W. and Eyre, T. **Advanced Simulation Environment for Induced Seismicity Mitigation and Integrated Control (ASEISMIC)**
3. Eyre, T. and Eaton, D.W. **Role of fault creep on earthquake nucleation in the Duvernay**
4. Igonin, N. and Eaton, D.W. **Bilinear magnitude distributions and the characteristic earthquake hypothesis**
5. Kao, H. **Improvement of Regional Seismograph Networks in Northeast BC and Western AB: Impact on Regulations of Unconventional Hydrocarbon Development**
6. Mahani, A.B. **Near-Field Ground-Motion Amplitudes from Induced Earthquakes in the Western Canada Sedimentary Basin**
7. Stork, A.L, Davey, I. and Grundy, J. **Hydraulic Fracturing: A Regulatory Perspective for England**



Monitoring of Anthropogenic Seismicity in Italy: State of the Art

Thomas Braun, INGV-Rome (IT), thomas.braun@ingv.it

Simone Cesca, GFZ-Potsdam (DE), simone.cesca@gfz-potsdam.de

Torsten Dahm, GFZ-Potsdam (DE), torsten.dahm@gfz-potsdam.de

Stefania Danesi, INGV-Bologna (IT), stefania.danesi@ingv.it

Andrea Morelli, INGV-Bologna (IT), andrea.morelli@ingv.it

Abstract

In Italy, the discussion about anthropogenic seismicity started after the deadly M6 Emilia earthquakes in 2012. Occurring these events in an area of gas and oil production, the question raised, whether stress perturbations induced by the exploitation may have triggered these events. In 2014, the Government published monitoring guidelines (ILG) describing regulations regarding hydrocarbon extraction, wastewater injection and CO₂ storage. The ILG prescribe the monitoring of pore pressure, microseismicity and ground deformation near sites of industrial activity and direct the application of a four-stage traffic light protocol. INGV has been charged to apply the ILG in three test areas and to provide indications about the applicability of these guidelines. We give a general overview about the state of the art, trying to emphasize critical situations as e.g. problems in magnitude calculation or traffic light thresholds, especially in areas with multiple mining rights.

Introduction

Since hydrofracking is used for shale gas production, human induced seismicity has become a subject of increasing interest, especially in the US and Canada (Ellsworth, 2013). As the Italian geology is not characterized by formations appropriate for shale gas exploitation, the discussion about anthropogenic seismicity in Italy was “triggered” for the first time after the deadly M_w6.2 Emilia earthquake in May 2012 (Scognamiglio et al., 2012; Cesca et al., 2013a). Since this seismic sequence occurred in vicinity of gas and oil production sites, the question raised, whether variations in crustal stressing accompanying the hydrocarbon exploitation may have influenced the generation of these earthquakes. As a first consequence, an International Commission on Hydrocarbon Exploration and SEismicity (ICHESE) was charged to investigate whether the 2012 earthquake sequence was induced or triggered by industrial activities in the area. The ICHESE-commission argued that only the Cavone oilfield and the Casaglia geothermal field were located in the vicinity of the main shocks, concluding that the stress change in the upper crust generated by their activity was most likely too small to have induced a seismic event, but that earthquake triggering could not be completely excluded (Astiz et al., 2014; Dahm et al., 2015). The final recommendation of the ICHESE-report was that all the existing and future activities of hydrocarbon exploitation (oil- and gas-production, wastewater reinjection), gas storage, geothermal energy production

will have to be subject of monitoring by high-quality networks, concerning seismicity, ground deformation and pore pressure variations.

Italian Guidelines for Monitoring effects of Industrial activity on the subsurface

In 2014, the Superior Institute of Environmental Protection and Research published a report about documented and hypothesized cases of triggered or induced seismicity in Italy (Fig. 1). Based on this re-

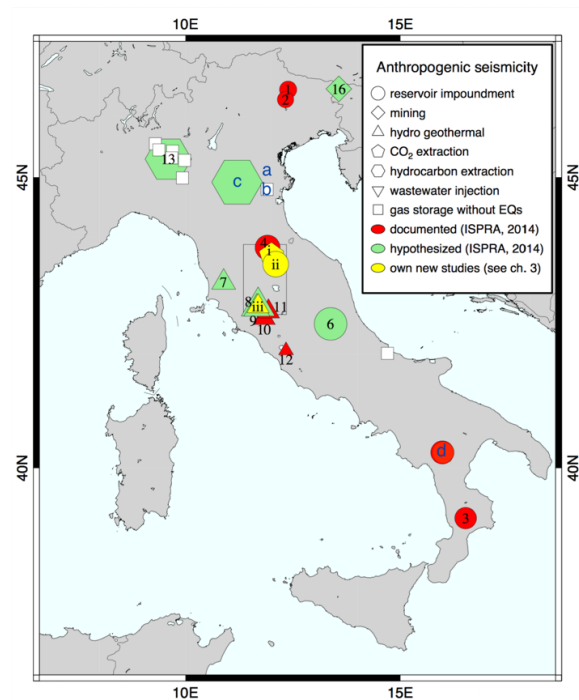


Fig. 1: Documented and hypothesized case of triggered and induced seismicity in Italy (Braun et al., 2018b).

port and on behalf of the Directorate-General for Safety of Mining and Energy Activities – National Mining Office for Hydrocarbons and Geo-Resources a group of experts compiled the “Italian Guidelines for monitoring the seismicity, underground deformation and pore pressure” (ILG, Dialuce et al., 2014). The ILG describe the governmental regulations, especially regarding hydrocarbon exploitation wastewater injection, and CO₂ storage. A more recent edition of the ILG concerning geothermal energy production was issued in 2016 (Terlizzese, 2016). Both guidelines prescribe standards for monitoring pore pressure, micro-seismicity and ground deformation and direct the application of a four-stage traffic light protocol, depending on magnitude, PGV and PGA. The ILG demand to report all events of $M_{max} \leq M_L 1.5$ (green), to reanalyze parameters and for $M_{green} \leq M_{max} \leq 2.2$ (yellow), to reduce production for $M_{green} \leq M_{max} \leq 3.0$ (orange), and to immediately halt industrial operations in case of events with $M_{orange} < M_L$ (red).

Experimental application of the ILG

In a three-years experimental phase, the ILG will now be applied in at least four different test areas:

- (i) Casaglia (Emilia Romagna, N-Italy) for low-enthalpy geothermal energy production.
- (ii) Minerbio (Emilia Romagna, N-Italy) for gas storage;
- (iii) Cavone (Emilia Romagna, N-Italy) for hydrocarbon exploitation/waste water reinjection;
- (iv) Val d’Agri (Basilicata, S-Italy).

In Italy hydraulic fracturing is not practiced, not only because the appropriate shale gas formation is lacking, but also because the technical commission of the Ministry of the Environment outlawed the use of any type of fracking technology for hydrocarbon exploitation (Zaratti, 2013).

Monitoring of Anthropogenic Seismicity in Italy

The National Institute of Geophysics and Volcanology (INGV) has been charged of managing multi-parametric monitoring systems, or to act as an evaluation agency, in these test areas, and to provide indications about the application of these guidelines (Fig. 2).

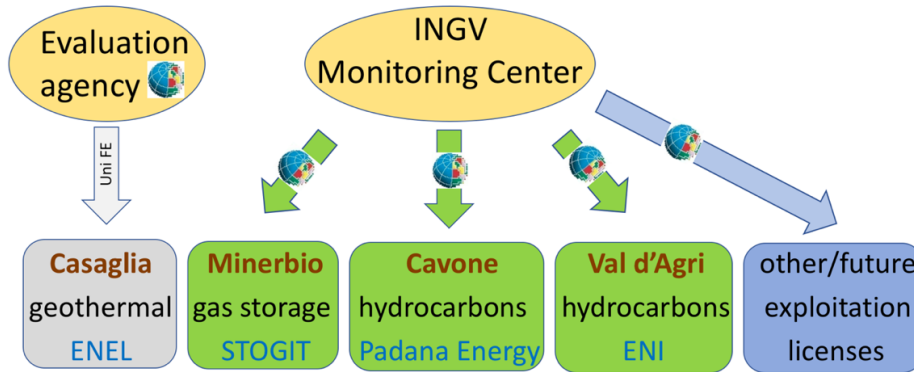


Fig. 2: Experimental application of the Governmental Monitoring Guidelines (ILG).

Some remarks on the application of the ILG

Based on recent experiences made e.g., in the geothermal area of Torre Alfina/Castel Giorgio, where in 2016 a M_L 4.1 earthquake occurred months before starting the geothermal exploitation (Fig. 3a), some annotations concerning the ILG can already be outlined:

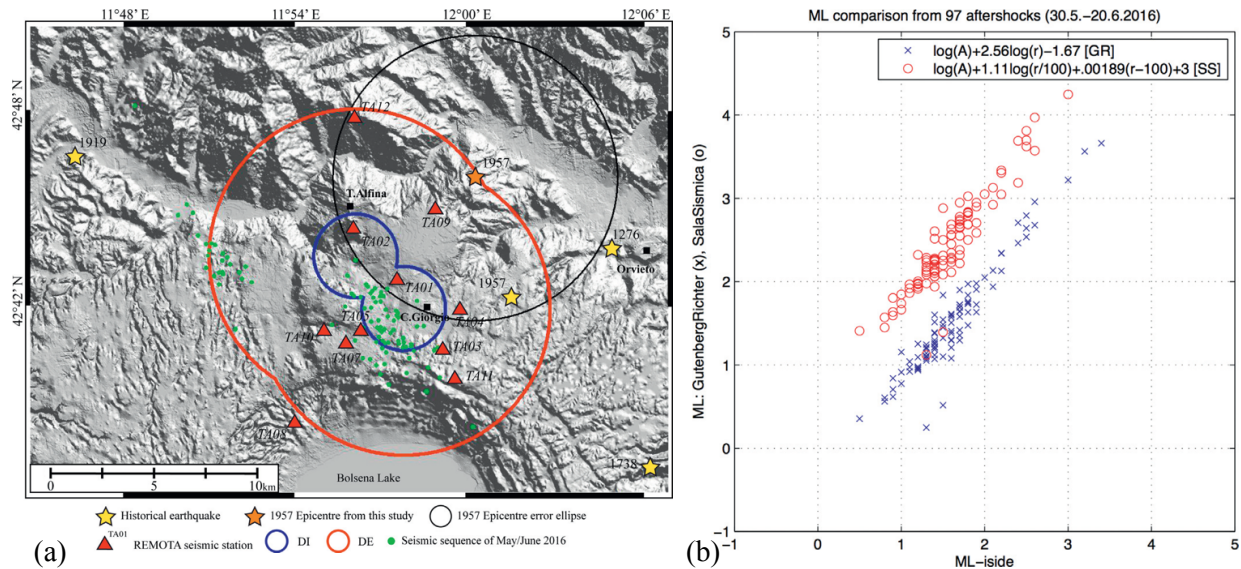


Fig. 3: The 2016 seismic sequence ($M_{max}=4.1$) at Castel Giorgio: (a) epicenters (green dots) with respect to the inner domain (blue line) and outer domain (red line) ; (b) comparison of the magnitudes determined of the local and the national seismic networks (from Braun et al., 2018a).

Monitoring of Anthropogenic Seismicity in Italy

One critical question is that companies with new licenses are obligated to realize a one-year monitoring period before starting the industrial operations (zero-line), which is indeed impossible for already existing concessions, producing since decades. With the forthcoming opening of the geothermal market in Tuscany many new concessions are expected to be situated inside or in the direct vicinity of the traditional areas of the main national energy producer, not excluding cases where different companies access the same reservoir. Here the question rises whether the requirement to determine the zero-line is reasonable. Another critical point of the ILG is the lack of any political consequence regarding the future production, in case that the natural seismicity exceeds the magnitude threshold already during the zero-line period. A further remark concerns the magnitude determination; in this regard the ILG do not specify the magnitude type to be calculated. Seismicity recorded by a local network at a future geothermal production site at Torre Alfina (12 in Fig. 1, Fig. 3a) shows that the M_L estimations are mostly incompatible with magnitudes determined by the National Seismic Network (Fig. 3b). Such differences are due to inaccurate attenuation laws and correction factors, especially for stations at local distances. In these conditions, the M_L becomes poorly constrained and should be better replaced by the more significant PGA and PGV.

Conclusions

Beyond the monitoring purposes, the experimental application of the ILG offers the great opportunity to access high quality data allowing to outline criteria for the discrimination between natural and anthropogenic seismicity. One of these might be to invert the full moment tensor also for low magnitude events (Cesca et al., 2013b); a further criterion could be to verify the hypocentral depth by alternative methods, as e.g., depth phase modeling by comparing synthetic array beams with the beam-trace of teleseismic array data (Fig. 4, Braun et al., 2018a).

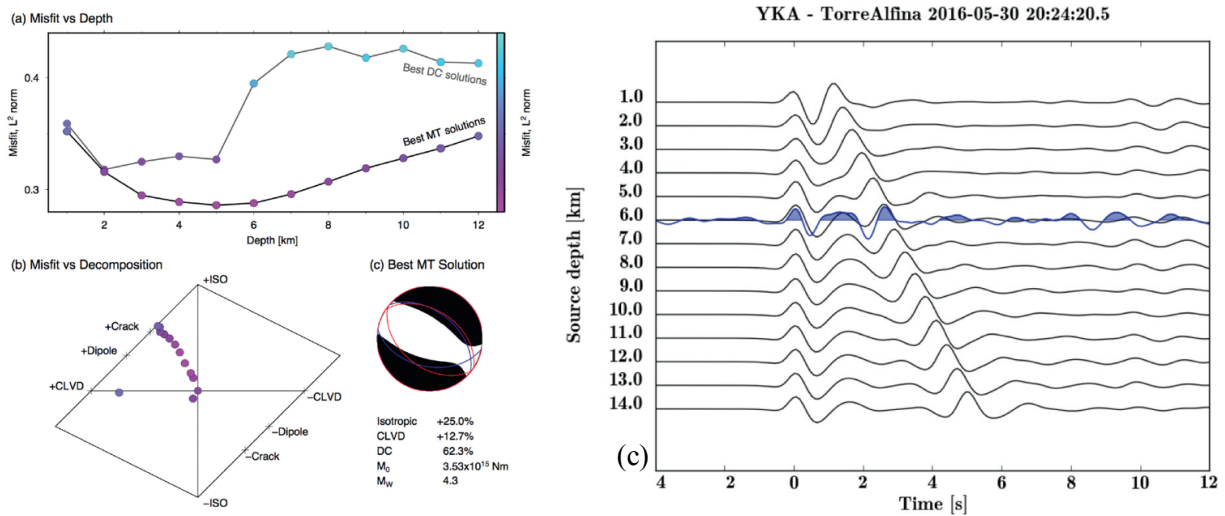


Fig. 4: Moment tensor inversion of the 30th May 2016 main shock (M_w 4.3) computed using waveforms within 100 km of epicentral distance. (a) misfit versus depth, assuming a DC source model (gray line) and full MT model (black line); (b) source-type diagram according to Hudson et al. (1989); (c) Array beam modelling using the Yellowknife-Array (YKA) (from Braun et al., 2018a)

Acknowledgements

Data from the seismic network at Torre Alfina geothermal field were collected in the framework of a research contract between INGV and ITW & LKW Geotermia Italia spa. The research was financed by Accordo Operativo 2018-19 INGV - MISE/DGS-UNMIG and co-financed by Project DPC Allegato B2-1 Task B 2018 (n° 0304.023).

References

- Astiz, L., Dieterich, J., Frohlich, C., Hager, B., Juanes, R., Shaw, J., 2014. On the Potential for Induced Seismicity at the Cavone Oilfield: Analysis of Geological and Geophysical Data, and Geomechanical Modeling. Technical Report. Report for the Laboratorio di Monitoraggio Cavone. <http://labcavone.it/documenti/32/allegatrapporto-studiogiacimento.pdf>.
- Braun, T., Caciagli, M., Carapezza, M., Famiani, D., Gattuso, A., Lisi, A., Marchetti, A., Mele, G., Pagliuca, N.M., Ranaldi, M., Sortino, F., Tarchini, L., Kriegerowski, M., and Cesca, S., 2018a. The seismic sequence of 30th May - 9th June 2016 in the geothermal site of Torre Alfina (central Italy) and related variations in soil gas emissions. *J. Volcanol. Geotherm. Res.* 359, pp. 21-36. 10.1016/j.jvolgeores.2018.06.005.
- Braun, T., Cesca, S., Kühn, D., Martirosian-Janssen, A. and Dahm, T., 2018b. Anthropogenic seismicity in Italy and its relation to tectonics: State of the art and perspectives. *Anthropocene*, 21, pp.80-94. 10.1016/j.ancene.2018.02.001.
- Cesca, S., Braun, T., Maccaferri, F., Passarelli, L., Rivalta, E., and Dahm, T., 2013a. Source modelling of the M5-6 Emilia-Romagna, Italy, earthquakes (2012 May 20-29). *Geophys. J. Int.*, 193, 1658-1672, doi:10.1093/gji/ggt069.
- Cesca, S., Rohr, A., and Dahm, T., 2013b. Discrimination of induced seismicity by full moment tensor inversion and decomposition. *J. Seismol.*, 17, pp.147-163. doi:10.1007/s10950-012-9305-8.
- Dahm, T., Cesca, S., Hainzl, S., Braun, T. and Krüger, F., 2015. Discrimination between induced, triggered and natural earthquakes close to hydrocarbon reservoirs: A probabilistic approach based on the modeling of depletion-induced stress changes and seismological source parameters. *J. Geophys. Res.* B2 120, pp. 2491-2509. 10.1002/2014JB011778.
- Dialuce, G., Chiarabba, C., Di Bucci, D., Doglioni, C., Gasparini, P., Lanari, R., Priolo, E., Zollo, A., 2014. Indirizzi e linee guida per il monitoraggio della sismicità, delle deformazioni del suolo e delle pressioni di poro nell'ambito delle attività antropiche. GdL MISE, Roma. unmig.mise.gov.it/unmig/agenda/upload/85_238.pdf.
- Ellsworth, W., 2013. Injection-induced earthquakes. *Science* 341, doi: 10.1126/science.1225942.
- Hudson, J., Pearce, R., Rogers, R., 1989. Source type plot inversion of the moment tensor. *J. Geophys. Res.* 94, 765-774.
- Scognamiglio, L., Margheriti, L., Mele, F.M., Tinti, E., Bono, A., De Gori, P., Lauciani, V., Lucente, F.P., Mandiello, A.G., Marcocci, C., Mazza, S., Pintore, S., Quintiliani, M., 2012. The 2012 Pianura Padana Emiliana seismic sequence: locations, moment tensors and magnitudes. *Ann. Geophys.* 55 (4), 549-559. <http://dx.doi.org/10.4401/ag-6159>.
- Terlizzese, F., 2016, Ottobre. Linee guida per l'utilizzazione della risorsa geotermica a media e alta entalpia. GdL MISE, Roma. <http://unmig.mise.gov.it/unmig/geotermia/lineeguida.pdf>.
- Zaratti, F., 2013. Italian Law n. 7-00073 presented by SEL, on 24.07.2013), approved as (n. 8-00012).



Advanced Simulation Environment for Induced Seismicity Mitigation and Integrated Control (ASEISMIC)

David W.S. Eaton, Department of Geoscience, University of Calgary eatond@ucalgary.ca

Thomas Eyre, Department of Geoscience, University of Calgary thomas.eyre@ucalgary.ca

Summary

Efforts to quantify induced-seismicity risk and to develop effective mitigation strategies are hampered by a dearth of numerical schemes that can accommodate realistic Earth models, while capturing the full spectrum of applicable physics. ASEISMIC is a new computational toolbox that is under development; it is designed to aid in preparing mitigation and response plans by combining reservoir-simulation methods with advanced geomechanical and seismological computational tools. The toolbox includes modules for site-specific induced seismicity operational risk assessment, by accessing relevant public data sources and augmenting those with additional, site-specific information.

This poster describes a new module within the ASEISMIC computational framework, called Poroelastic Regional Stress Simulation (PReSS). Stresses acting in the subsurface have a very strong influence on well completion activities such as hydraulic fracturing, as well as activation of pre-existing faults (induced seismicity). The influence of lithologic layering is often not considered and it is further often assumed that the presence of a fault has negligible effect on the background stresses. These effects are considered here within the linear poroelastic framework subject to the following basic assumptions: 1) the failure criterion is based on a linear Mohr-Coulomb relationship that incorporates cohesion and representation of a near-critical (*pericritical*) stress state using a fault stability margin parameter; 2) stresses in each layer are calculated under a state of uniform horizontal elastic strain; 3) faults are represented as tabular zones of weakness that give rise to low-stress inclusions. The figure below shows an example of a stratified stress field computed based on well log data from the Kaybob-Duvernay region in western Canada. Model parameters have been adjusted to fit available pore-pressure and S_{hmin} data. The target interval for hydraulic fracturing, at ~3440-3480 m depth, is close to a critically stressed state due to elevated pore pressure values. The areas of greatest stress correspond to mechanically strong layers characterized by a relatively high static Young's modulus.

Acknowledgements

This work was supported by the Canada First Research Excellence Fund (CFREF) through the Global Research Initiative in Sustainable Low Carbon Unconventional Resources program at the University of Calgary.

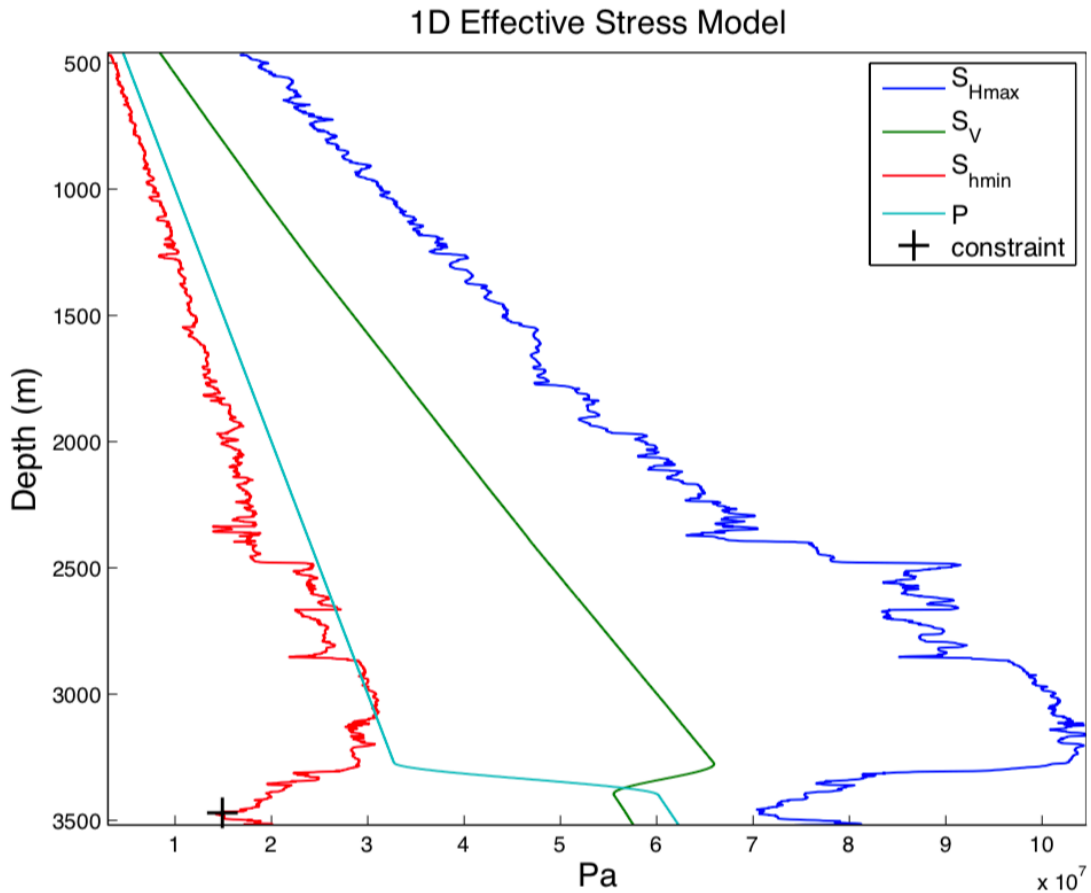


Figure 1: Stratified effective stress model computed for a well in western Canada (01-36-61-22 W5). Mechanical properties (Young's modulus, Poisson's ratio and density) were derived from well logs and converted from dynamic to static values using the regression parameters from Slota-Valim (2015). A fault slip margin of 4.0 MPa and Biot parameter $\alpha = 0.5$ were assumed. The pore-pressure profile (P) is based on Eaton and Schultz (2018) and the constraint on S_{hmin} was calculated using a regional gradient of 22 kPa/m from Fox and Soltanzadeh (2015).

References

- Eaton, D.W. and Schultz, R., 2018. Increased likelihood of induced seismicity in highly overpressured shale formations. *Geophysical Journal International*, 214(1), 751-757.
- Fox, D. A., and M. Soltanzadeh (2015). A regional geomechanical study of the Duvernay Formation in Alberta, Canada, GeoConvention 2015: New Horizons, Calgary, Alberta, available at https://www.geoconvention.com/archives/2015/350_GC2015_A_Regional_Geomechanical_Study_Duvernay_Formation.pdf (last accessed April 2018).
- Slota-Valim, M., 2015. Static and dynamic elastic properties, the cause of the difference and conversion methods—case study. *Nafta-Gaz*, 11, 816-826.



Role of fault creep on earthquake nucleation in the Duvernay

Thomas S. Eyre, Department of Geoscience, University of Calgary thomas.eyre@ucalgary.ca

David W.S. Eaton, Department of Geoscience, University of Calgary eatond@ucalgary.ca

Dmitry I. Garagash, Department of Civil and Resource Engineering, Dalhousie University Garagash@dal.ca

Marco Venieri, Department of Geoscience, University of Calgary marco.venieri@ucalgary.ca

Ronald Weir, Department of Geoscience, University of Calgary ronald.weir@ucalgary.ca

Summary

Models for hydraulic-fracturing induced earthquakes in shales typically ascribe fault activation to elevated pore pressure or increased shear stress (*Bao & Eaton, 2016*). Seismicity up to M_w 4.1 has been correlated with hydraulic-fracturing operations targeting the Duvernay formation, western Canada (*Atkinson et al., 2016*). High resolution microseismic monitoring of treatments associated with the induced seismicity indicate that the earthquakes tend to nucleate over relatively short injection timescales and sufficiently far from the injection zone, making triggering by either poroelastic stress changes or pore pressure diffusion unlikely. These mechanisms are also incompatible with experiments and rate-state frictional models, which predict stable sliding (aseismic slip) on faults that penetrate rocks with high clay or total organic content (*Guglielmi et al., 2015; Kohli & Zoback, 2013*). We introduce a new model, where unstable regions of a fault are progressively loaded by aseismic creep accelerated by fluid injection. The creep front significantly outpaces the pore pressure diffusion front and supports the timescales of earthquake nucleation observed. This model provides a better fit to the data, including spatiotemporal evolution of seismicity in relation to formation lithologies (which are consistent with predictions of regions of stable sliding (aseismic creep) and unstable slip (seismic rupture) according to rate-state frictional models), and the long-lived seismic swarms identified at some treatments. Dynamic weakening of the fault gouge is essential for a large earthquake to be induced, therefore carbonates are most susceptible due to the propensity for flash-heating-induced thermal decomposition of calcite (*Han et al., 2007*). In a broader context, the apparent association of hydraulic fracturing induced seismicity with faulting in carbonates is consistent with observations of some of the largest natural earthquakes occurring within the sedimentary cover worldwide (*Chen et al., 2015*). Improved understanding of the fundamental processes of fault activation during hydraulic-fracturing is key to developing effective monitoring and mitigation strategies and could also help to inform models for natural earthquake triggering.

Acknowledgements

The authors are very grateful to Repsol Oil & Gas Canada Inc. for providing the microseismic data, which were processed by Magnitude. In addition, TGS Canada Corp. is thanked for providing the 3D multicomponent data used in this study. TOC data were measured by Weatherford and XRD data were collected by Chevron; these data were sourced from the Alberta Energy Regulator database. This research was supported in part by funding from the Canada First Research Excellence Fund and from Discovery Grant 05743 by Natural Science and Engineering Research Council to D.I.G. We thank the sponsors of the Microseismic Industry Consortium and CREWES for their financial support of this study.

References

- Atkinson, G.M., Eaton, D.W., Ghofrani, H., Walker, D., Cheadle, B., Schultz, R., Shcherbakov, R., Tiampo, K., Gu, J., Harrington, R.M. and Liu, Y., 2016. Hydraulic fracturing and seismicity in the Western Canada Sedimentary Basin. *Seismological Research Letters*, 87(3), 631-647.
- Bao, X., and Eaton, D.W., 2016. Fault activation by hydraulic fracturing in western Canada. *Science*, 354(6318), 1406-1409.
- Chen, J., Verberne, B.A., and Spiers, C.J., 2015. Effects of healing on the seismogenic potential of carbonate fault rocks: Experiments on samples from the Longmenshan Fault, Sichuan, China. *Journal of Geophysical Research*, 120, 5479–5506.
- Guglielmi, Y., Cappa, F., Avouac, J.P., Henry, P., and Elsworth, D., 2015. Seismicity triggered by fluid injection–induced aseismic slip, *Science*, 348(6240), 1224-1226.
- Han, R., Shimamoto, T., Hirose, T., Ree, J.-H., and Ando, J.I., 2007. Ultralow friction of carbonate faults caused by thermal decomposition. *Science*, 316, 878–881.
- Kohli, A.H., and Zoback, M.D., 2013. Frictional properties of shale reservoir rocks. *Journal of Geophysical Research*, 118(9), 5109-5125.



Banff 2018 International Induced Seismicity Workshop

October 24 – 27, 2018

Bilinear magnitude distributions and the characteristic earthquake hypothesis

Nadine Igonin, Department of Geoscience, University of Calgary, naigonin@ucalgary.ca

David W.S. Eaton, Department of Geoscience, University of Calgary eatond@ucalgary.ca

Summary

Magnitude frequency distributions obtained from induced seismicity are often assumed to obey a Gutenberg-Richter (G-R) relationship. For most applications, this seems to be accurate, but we present here an unusual case where there appears to be a bilinear magnitude distribution. The Tony Creek dual Microseismic Experiment (ToC2ME) is a passive seismic dataset obtained during hydraulic fracturing near Fox Creek, Alberta (Eaton et al., 2018). The treatment resulted in several events over Mw 1.5, with the largest event being Mw 3.2. Figure 1 shows a map of the recorded seismicity and the magnitude frequency distribution for the catalog of the 4,000 largest events. There is a clear bilinear trend, with an anomalously low apparent b value of 0.6 and a secondary b value of 1.6. The b value of 1.6 can be attributed to the superposition of separate clusters with b values of ~ 1 and ~ 2 . To explain the usual b value of 0.6, we invoke the characteristic earthquake hypothesis, which posits that although an earthquake system behaves in a G-R way in between cycles, there occur on occasion larger characteristic earthquakes (Wesnousky, 1994). These earthquakes are the largest the system can produce, and would explain the statistically unexpected high number of events over Mw 2.0. Individual clusters in the dataset appear to exhibit such behaviour, and the regional catalog for this area also has an unusually low b value of 0.63. We suggest that the superposition of these characteristic earthquakes results in the low b value, and that bilinear distributions, and characteristic earthquakes, may be a more common trend than previously thought.

Acknowledgements

The ToC2ME program was enabled by generous support from two companies. Continuous raw data (geophone and broadband recordings, network code TC2ME) are available through the IRIS data center at <http://ds.iris.edu/mda/5B?timewindow=2016-2017>, following a holdback period that expires on July 1, 2020. Financial support was provided by Chevron and the Natural Sciences and Engineering Research Council of Canada (NSERC) through the NSERC-Chevron Industrial Research Chair in Microseismic System Dynamics. Continuous geophone data were recorded under license from Microseismic Inc. for use of the BuriedArray method. All sponsors of the Microseismic Industry Consortium are also sincerely thanked for their ongoing support.

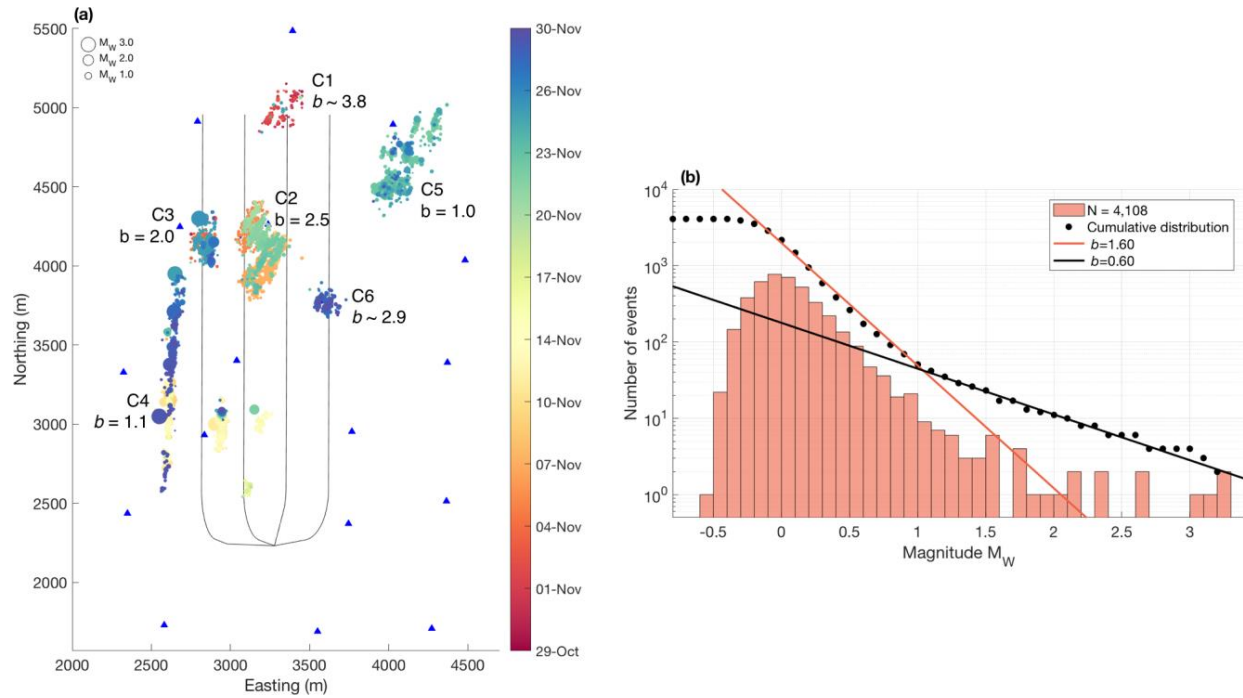


Figure 1: Overview of ToC2ME locations and magnitude distribution. (a) Map of hydraulic fracturing wells (black lines), a subset of the 68-station array (blue triangles), and the microseismic events recorded, coloured in time. Clusters and their corresponding b values are labelled, with b values that have been obtained from small catalog sizes equated with a '~'. (b) Magnitude frequency distribution for the whole dataset.

References

- Eaton, D., N. Igonin, A. Poulin, R. Weir, H. Zhang, S. Pellegrino, and G. Rodriguez, 2018. Induced seismicity characterization during hydraulic fracture monitoring with a shallow-wellbore geophone array and broadband sensors, *Seismological Research Letters*, doi:10.1785/0220180055.
- Wesnousky, S. G., 1994. The Gutenberg-Richter or characteristic earthquake distribution, which is it?, *Bulletin of the Seismological Society of America*, 84(6), 1940–1959.

Improvement of Regional Seismograph Networks in Northeast BC and Western AB: Impact on Regulations of Unconventional Hydrocarbon Development

Honn Kao, Geological Survey of Canada, Natural Resources Canada, Honn.Kao@canada.ca

Summary

By establishing close collaborations with many partners, including regulators, government research organizations, universities, professional societies, and the energy industry, significant improvement has been made to enhance the earthquake monitoring capability of regional seismograph networks in northeast BC and western AB. As a result, the overall magnitude of completeness of the regional earthquake catalogue has been improved by about one magnitude unit, dropping from $M_L \geq 2.5$ to ~ 1.5 . The improved earthquake monitoring has dramatically enhanced the performance of regulatory agencies by allowing regulators to: 1) better identify and define “sweet spots” of IIE; 2) strengthen earthquake monitoring requirements for specific sites; 3) rapidly respond to media and public inquiries about possible felt injection-induced events; and 4) understand the full impact/consequence of ground shaking caused by individual induced events.

Introduction

Northeast BC and western AB are part of the Western Canada Sedimentary Basin that hosts the biggest unconventional hydrocarbon production in Canada. The development of unconventional hydrocarbon resources in the region first started in 2006 when the station density of the Canadian National Seismograph Network (CNSN) was very sparse (Farahbod et al., 2015). Consequently, many injection-induced earthquakes (IIE) that were associated with hydraulic fracturing (HF), wastewater disposal, or enhanced recovery, were not properly detected and located due to the network’s detection limit.

Recognizing this important knowledge gap, Natural Resources Canada (NRCan) initiated the Induced Seismicity Research (ISR) Activity in 2012, later expanded and became the ISR Project in 2016, to investigate the source characteristics and seismogenic conditions of IIE. By establishing close collaborations with many partners, including regulators, government research organizations, universities, professional societies, and the energy industry, significant improvement has been made to enhance the earthquake monitoring capability of the regional seismograph network in northeast BC and western AB. A large number of new broadband stations were established and all the real-time seismic waveform data are archived at the Data Management Center of the Incorporated Research Institutions for Seismology (IRIS-DMC) for immediate release. There are also dense arrays established by universities and individual operators that provide high-resolution monitoring for specific areas of interest.

In this presentation, I will first describe the various efforts to densify the regional seismograph networks in western Canada with a special reference to the Western Canada Sedimentary Basin. Then, I will briefly describe major research collaboration initiatives aiming at understanding the source process of IIE and the associated seismic hazards. Finally, I will summarize the positive impact of the improved regional seismograph networks on regulatory performances and the development of new regulations as a result of increased understanding of the physical processes of induced seismicity.

Densification of Regional Seismograph Networks

Figure 1 shows the regional seismicity and distribution of real-time seismograph stations in western Canada in the pre-development era (i.e., before late 2006, Figure 1a) and now (Figure 1b). In 2006, the Canadian National Seismograph Network (CNSN), operated by NRCan for routine earthquake monitoring, had only a handful of real-time station in northeast BC and western AB. The overall earthquake magnitude of completeness is estimated at $M_L \sim 2.5$.

With close collaborations among regulators, government research organizations, universities, professional societies, and the energy industry (a topic to be presented in more detail in the next section), a series of efforts

Improvement of Regional Seismograph Networks in Western Canada

were made since 2013 to densify the real-time seismic station coverage in the unconventional hydrocarbon production region. Most significant contributions include 8 new stations established by the BC Seismic Research Consortium, 21 by Alberta Geological Survey (the RAVEN network), 27 by the Canadian Induced Seismicity Collaboration (the TransAlta network), 4 by Yukon Geological Survey, 7 by University of Ottawa, and a dense seismic array consisting of 9 stations by McGill University in the Dawson Creek area. Real-time waveform data from all these stations, except the TransAlta network, are transmitted back to the VSAT hub at the Sidney office of the Geological Survey of Canada (GSC) for real-time analysis. A separated data stream goes to IRIS-DMC for data archiving and distribution. The latest effort is made by BC Oil and Gas Commission (BCOGC) and NRCan to establish 9 new stations at strategic locations co-sited with both broadband and strong-motion sensors. Seven such stations are in operation and the two remaining ones will be installed in early 2019.

Overall, the earthquake magnitude of completeness has been improved by one magnitude unit from $M_L \sim 2.5$ to 1.5 (Babaie Mahani et al., 2016; Kao et al., 2018a). The number of earthquakes that can be detected and located with the combined dataset has dramatically increased as well. Taking the period of January 2014–December 2016 for example, the NRCan ISR Project reported more than 4900 events using the combined dataset, about 4 times larger than the NRCan routine earthquake catalogue (Visser et al., 2017).

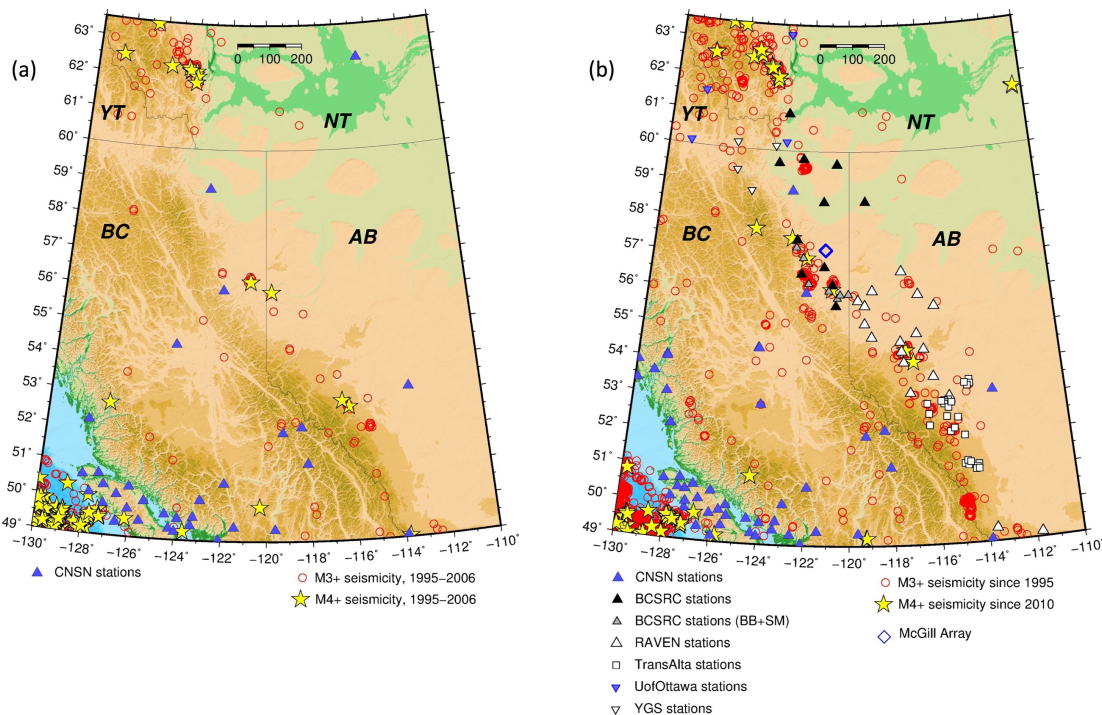


Fig. 1. Maps showing the regional seismicity and distribution of real-time seismograph stations in western Canada. (a) and (b) correspond to the year of 2006 and 2018, respectively.

Development of Collaborations

Microseismicity Industry Consortium

This consortium was established in 2010 with a large number of industry sponsors and the NSERC Industrial Research Chair funding to University of Calgary (Prof. D. Eaton). It is co-led by Prof. D. Eaton of University of Calgary and Prof. M. van der Baan of University of Alberta. The vision of this consortium is to take a multidisciplinary approach to conduct research related to microseismicity data acquisition, processing and interpretation. Specific research goals and objectives are developed over time in close consultation with industry sponsors. More information can be obtained at the Consortium's website at www.microseismic-research.ca.

Improvement of Regional Seismograph Networks in Western Canada

BC Seismic Research Consortium (BCSRC)

The BCSRC was established in 2012 under an MOU among four original members: GSC/NRCan, BCOGC, Geoscience BC, and the Canadian Association of Petroleum Producers (CAPP). The Yukon Geological Survey joined the BCSRC in 2016 to become the latest member. The primary objective of BCSRC is to form a framework for research co-operation to study induced seismicity in northeastern BC. It has three main tasks: 1) densify the regional seismic network in the unconventional hydrocarbon production areas, 2) promote research of induced seismicity related to the development of unconventional hydrocarbons, and 3) facilitate data sharing and information exchange related to the study of induced seismicity.

Canadian Induced Seismicity Collaboration

This research collaboration organization was established in 2014 based on an Industrial Research Chair funded by NSERC and two industrial partners (TransAlta and Nanometrics) and a NSERC Collaborative Research and Development grant to Western University (Prof. G. Atkinson). Partners include University of Calgary, Alberta Geological Survey/Alberta Energy Regulator (AER), GSC/NRCan, University of Alberta, and McGill University. The primary purpose of this organization is to coordinate research efforts focusing on understanding the mechanisms and seismic hazards associated with industry-related induced seismicity. Specific tasks include the expansion of seismic network in Alberta and the promotion of research collaborations on hazards from induced seismicity and induced seismicity processes. More information can be obtained at the organization's website at www.inducedseismicity.ca.

NSERC Strategic Partnership for Induced Earthquake Research

This project is funded by a NSERC Strategic Research grant to McGill University (Prof. Y. Liu and Prof. R. Harrington) for 4 years (2016–2020). This strategic partnership was initially formed between McGill University and GSC/NRCan, and later expanded with the participation of BCOGC. It aims at coordinating research efforts on induced seismicity in specific target areas in BC. Multidisciplinary research projects were proposed to study detailed source processes of induced events, including establishing a dense seismic array in the high HF activity area near Dawson Creek, ground deformation studies using InSAR and GPS data, and monitoring and analysis of groundwater chemistry.

Comprehensive Ground Motion Monitoring Network in Northeast BC

This collaboration was established between BCOGC and GSC/NRCan with in-kind support from the oil and gas industry. The main objective of this project is to better characterize the ground motion distribution of induced earthquakes in BC and their potential seismic hazards. Nine new seismograph stations, each is equipped with one broadband seismometer and one accelerometer, are established at strategic locations to further enhance the regional earthquake monitoring capability. All seismic signals are transmitted back to the GSC Sidney office in real-time mode via high-speed cellular modems. The deployment of 7 stations were completed in September and October 2018. The remaining 2 stations will be done by early 2019.

Impact on Regulatory Performances

The improved regional seismograph networks provide much better constraint on epicentral locations. The improved earthquake monitoring has also dramatically enhanced the performance of regulatory agencies. Specifically, regulators can better identify and define the “sweet spots” of IIE. They can also take proactive steps to strengthen earthquake monitoring requirements for specific sites or areas. In case of a significant or felt IIE, they can rapidly respond to media and public inquiries with accurate information about the event's source parameters. And regulators now have reliable tools to assess the full impact/consequence of ground shaking caused by individual IIE events. Data from the improved regional seismograph networks also lead to a wealth of new insight into the delineation of possible controlling factors of IIE that can be adopted in new regulations for more effective mitigation of seismic hazards from IIE.

Development of New Regulations on Injection-Induced Earthquakes

The most significant development of regulations on IIE is the establishment of Induced Seismicity Traffic Light Protocol (IS-TLP) by provincial regulators. AER issued the Subsurface Order No. 2 on 19 February 2015 that requires all operators in the Fox Creek area to setup seismic monitoring array capable of detecting M_L 2+ events within 5 km of HF wells. A yellow light is triggered if an earthquake of M_L between 2 and 4 is observed. Operators

Improvement of Regional Seismograph Networks in Western Canada

triggering a yellow light are required to implement their predefined mitigation strategies in an attempt to limit the escalation of magnitudes. A red-light condition, which requires immediate suspension of injection operations, takes effect when an M_L 4+ earthquake is observed. Operators triggering a red light are not allowed to resume until receiving AER's approval and must submit their recorded seismic data. A technical workshop was held at the GSC Sidney office in October 2015 to discuss the effectiveness of IS-TLP with recommendations (Kao et al., 2016). A more detailed performance analysis of IS-TLP in BC and AB is given by Kao et al. (2018b)

In BC, the BCOGC implemented similar regulations for induced seismicity in June 2015, which were drafted based on permit conditions that were applied to well permits beginning in 2014. The regulations require permit holders to suspend their injection operations if an M_L 4 or larger earthquake occurs within 3 km of the well(s). Operations are allowed to resume only after a mitigation plan is submitted and approved by BCOGC. In June 2016, BCOGC introduced new permit conditions in an effort to measure the intensity of induced earthquakes by requiring the installation of seismic monitoring instruments in two "designated ground-motion monitoring" areas. The installed seismometers must be located within 3 km of the common drilling pad with a minimum detectability of 2% earth's gravity (g). Operators are also required to submit a ground-monitoring summary report within 30 days after the completion of HF activities and the recorded seismic data for any events with ground motion exceeding 2% g . In 2017, the Drilling and Production Regulation was amended to include induced seismicity associated with both HF and wastewater disposal operations (BCOGC Industry Bulletin 2017-10). In May 2018, BCOGC Special Project Order 18-19-001 was issued with monitoring, mitigation and reporting requirements for permit holders in the Kiskatinaw Seismic Monitoring and Mitigation Area (aka, the Farmington area).

Conclusions

1. Significant efforts have been made by governments, academia, and the energy industry to improve monitoring capability of regional seismograph networks in western Canada.
2. The magnitude of completeness for regional seismicity has been improved by one magnitude unit from M_L ~2.5 to 1.5, which is deemed appropriate for regulatory purposes.
3. Multidisciplinary research collaborations were proactively promoted to address critical knowledge gaps identified by regulators, the industry, and the research community.
4. As a result, regulatory performances are constantly improved with a balanced approach between economic benefit of unconventional resource development and the protection of public safety and environments.

References

- Babaie Mahani, A., Kao, H., Walker, D., Johnson, J., & Salas, C. (2016). Performance evaluation of the regional seismograph network in northeast British Columbia, Canada, for monitoring of induced seismicity. *Seismological Research Letters*, 87(3), 648-660. doi:10.1785/0220150241
- Farahbod, A. M., Kao, H., Walker, D. M., & Cassidy, J. F. (2015). Investigation of regional seismicity before and after hydraulic fracturing in the Horn River Basin, northeast British Columbia. *Can. J. Earth Sci.*, 52, 112-122. doi:10.1139/cjes-2014-0162
- Kao, H., Eaton, D. W., Atkinson, G. M., Maxwell, S., & Babaie Mahani, A. (2016). Technical meeting on the traffic light protocol (TLC) for induced seismicity: Summary and recommendations. *Geol. Surv. Canada Open-File Report*, 8075, 20pp. doi:10.4095/299002
- Kao, H., Hyndman, R., Jiang, Y., Visser, R., Smith, B., Babaie Mahani, A., . . . He, J. (2018a). Induced seismicity in western Canada linked to tectonic strain rate: Implications for regional seismic hazard. *Geophys. Res. Lett.*, in press.
- Kao, H., Visser, R., Smith, B., & Venables, S. (2018b). Performance assessment of the induced seismicity traffic light protocol for northeastern British Columbia and western Alberta. *The Leading Edge*. doi:10.1190/tle37020117.1.
- Visser, R., Smith, B., Kao, H., Babaie Mahani, A., Hutchinson, J., & McKay, J. E. (2017). A comprehensive earthquake catalogue for northeastern British Columbia and western Alberta, 2014–2016. *Geol. Surv. Canada Open-File Report*, 8335, 27pp. doi:10.4095/306292

Near-Field Ground-Motion Amplitudes from Induced Earthquakes in the Western Canada Sedimentary Basin

Alireza Babaie Mahani, Geoscience BC, ali.mahani@mahangeo.com

Near-field ground-motion amplitudes from 241 potentially induced earthquakes in the Western Canada Sedimentary Basin are analyzed in this study. First, I obtain moment magnitude (M) for the events without the reported M in the earthquake catalogue using vertical component of response spectral acceleration at 1.0 and 3.3 Hz. Events are within the M range of 1.0 to 4.6 with most events having focal depths between 3 and 4 km and recorded at hypocentral distance of as close as 1.6 km. It seems that the maximum horizontal motions (RotD100) are lower than the damage threshold at hypocentral distances > 5 km. At shorter distances, however, high-frequency motions (e.g. peak ground acceleration) may reach the damage threshold for the events with $M \geq 2.5$, suggesting that ground-motion amplitudes from induced earthquakes can become a high-frequency hazard. I also use a diverse group of ground motion prediction equations to test their validity with the observed motions.

Introduction

An important concern regarding induced seismicity from fluid injection is the potential for large ground-motion amplitudes that might be above the damage threshold of structures within areas of oil and gas activities. Whereas natural earthquakes with magnitudes ≥ 5 usually include the most share of seismic hazard, for induced earthquakes, magnitude of events may not be a proper justification as smaller earthquakes can generate large ground-motion amplitudes due to their shallow depths (Babaie Mahani and Kao, 2018). Recorded ground-motion amplitudes at near field from shallow induced earthquakes show that events with magnitudes in the range of 3 to 5 can be detrimental to structures, with reports of damage from Alberta, Texas, Oklahoma, and Kansas (Taylor et al., 2018). Here, I look at the ground-motion amplitudes from potentially induced earthquakes in WCSB that were mostly compiled from dense local seismograph networks within the oil and gas operating areas. I include 241 events in northeast British Columbia and western Alberta which were recorded within hypocentral distance < 50 km. Of particular interest are the characteristics of amplitudes at very short hypocentral distance (e.g. within 5 km). I also use a suite of ground motion prediction equations (GMPEs) to test the validity of these models with the observed ground-motion amplitudes.

Database

Waveforms from 241 potentially induced earthquakes recorded at hypocentral distances of 1.6 to 46 km were used in this study. Velocity time series were obtained after correcting each waveform for the instrument response and then filtered using a second-order, high-pass Butterworth filter with corner frequency of 0.1 Hz with the exception of one event for which a corner frequency of 0.5 Hz was chosen based on the visual inspection of the waveforms. Acceleration time series were then calculated through differentiation of the velocity time series. Three-component peak ground acceleration (PGA), peak ground velocity (PGV), and 5%-damped response spectral acceleration (PSA) for frequencies 0.3, 0.5, 1, 2, 3.3, 5, 10, 20, 33.3, and 50 Hz were obtained for all events. Figure (1) shows the distribution of events and seismograph stations.

I used the relation by Atkinson et al. (2014) which is based on the vertical PSA amplitudes at frequencies of 1.0 and 3.3 Hz to estimate M for events without the reported M in the earthquake catalogue. M for the events range between 1.0 and 4.6. For most events focal depth was calculated during the location process. However, there are events for which depth was either assigned a fixed value during the location process or an assumption made for the depth in this study. The majority of ground-motion amplitudes are at hypocentral distances of < 20 km and $M < 2.5$ with most of the events having focal depths reported between 3 and 4 km.

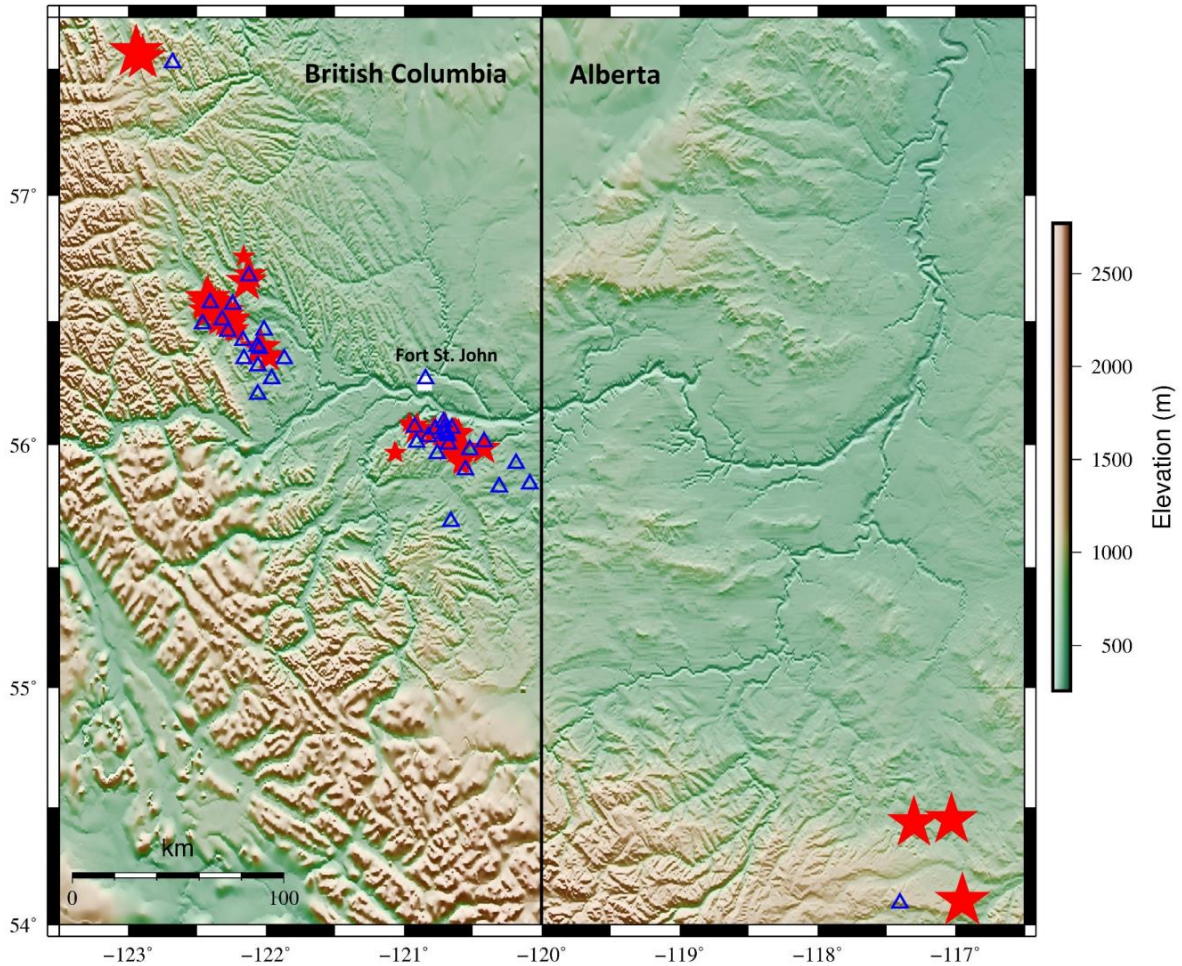


Fig. 1. Distribution of the events (stars) and seismograph stations (triangles).

Near-Field Ground Motion

Figure 2 shows the PSA values (RotD100; Boore, 2010) from events with $M \geq 2.5$ that were recorded in the hypocentral distance ranges of 0-5 (Figure 2a) and 5-10 km (Figure 2b). Also plotted are the mean ground-motion amplitudes associated with modified mercalli intensity (MMI) of 6, which can be indicative of the start of damage (Worden et al., 2012; Atkinson, 2017). It is clear in Figure 2 that ground-motion amplitudes from small earthquakes considered in this study are below the MMI 6 at the hypocentral distances of 5 to 10 km. At shorter distances, ground motions can reach the MMI 6 at high frequencies (e.g. PGA). As mentioned in Atkinson (2017), it seems that ground motions from small, induced earthquakes are only a high-frequency seismic hazard. This is because large, high-frequency ground motions from events with magnitude range considered in this study are usually from very short duration pulses (Babaie Mahani and Kao, 2018). In Figure 3, the bracketed duration (D_b ; Bommer and Martinez-Pereira, 1999) for the three-component waveforms is shown versus PGA and PGV. D_b was calculated for ground-motion amplitudes above the MMI 2 (1.4 cm/sec^2 and 0.06 cm/sec). Although, PGA can reach as high as MMI 6, the highest PGV lies between MMI 4 and 5. Since velocity is an integral of acceleration over time, in order to get large velocities, large accelerations must be sustained over longer period. For small magnitude earthquakes, although large accelerations can be observed, they are usually from short period spikes leading to small velocities. On the other hand, for large events, combination of large accelerations from long period pulses results in large velocities (Babaie Mahani and Kazemian, 2018).

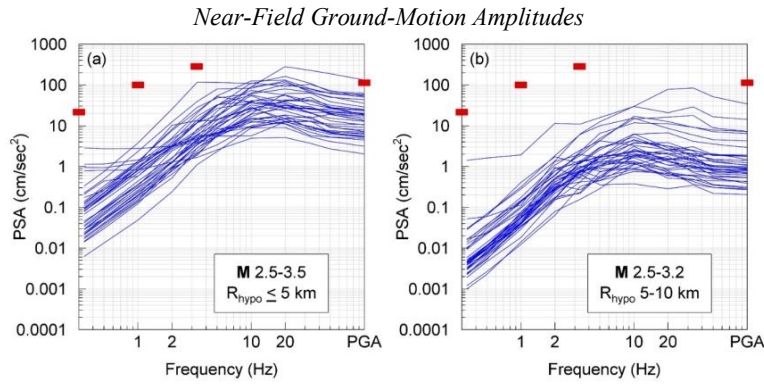


Fig. 2. Response spectral acceleration (PSA) for the maximum horizontal motion (RotD100) versus frequency. (a) PSA values from events with moment magnitude (M) 2.5-3.5 recorded at hypocentral distance (R_{hypo}) < 5 km. (b) PSA values from events with M 2.5-3.2 recorded at R_{hypo} between 5 and 10 km. Solid rectangles show the ground-motion amplitudes associated with the modified mercalli intensity of 6 based on relations provided by Worden et al. (2012).

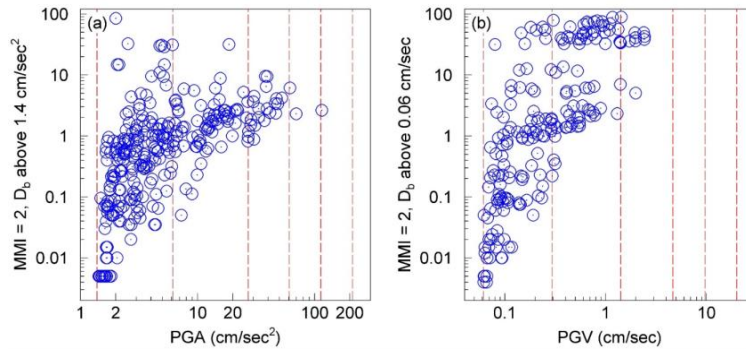


Fig. 3. Bracketed duration (D_b) for the three-component waveforms used in this study versus peak ground acceleration (PGA) and peak ground velocity (PGV). D_b was calculated for the acceleration and velocity time series for ground-motion amplitudes above 1.4 cm/sec^2 and 0.06 cm/sec , respectively, corresponding to the modified mercalli intensity (MMI) of 2 (Worden et al., 2012). Dashed lines show ground motions for MMI 2 to 7.

Comparison with GMPEs

In Figure 4 PGA values (RotD50), corrected for the B/C site condition ($V_{s30} = 760 \text{ m/sec}$), is shown versus hypocentral distance for different magnitude bins. To correct the ground-motion amplitudes to the reference site condition, site correction factors from Boore et al. (2014) was used. V_{s30} values were estimated based on the relationship between site fundamental frequency (f_{peak}) and V_{s30} . Using the averaged horizontal-to-vertical ratio of motion (geometric mean of the horizontal components to vertical component; H/V), the f_{peak} which is the frequency where the maximum H/V ratio occurs was estimated for each station. I then obtained V_{s30} using Hassani and Atkinson (2016) relationship for the central and eastern north America. Also plotted in Figure 4 are the attenuation curves that were obtained for other regions for either generic rock sites (McGarr and Fletcher, 2005, MF05, and Douglas et al., 2013, D13) or B/C site condition (Boore et al., 2014, B14, Atkinson, 2015, A15, and Yenier and Atkinson, 2015, YA15) for M 1.5, 2.5, 3.5, and 4.5. While MF05 and D13 were obtained from ground motions of $M \leq 4$ events, other models (B14, A15, and YA15) include ground motions from $M \geq 3$ events. For the small magnitude ranges (M 1.0-2.0 and 2.0-3.0) shown in Figure (4a and b), D13 seems to match the ground-motion amplitudes although there is an underestimation for short hypocentral distances. MF05 clearly underestimates PGA values for these magnitude ranges. For ground motions in the magnitude range of 3 to 4 (Figure 4c), while MF05 underestimates the PGA values, other models (D13, B14, A15, and YA15) appear to match the data well. For the largest magnitude range ($M > 4.0$; Figure 4d), there are not enough data to make a robust conclusion although it seems that B14, A15, and YA15 estimate the ground-motion amplitudes relatively well.

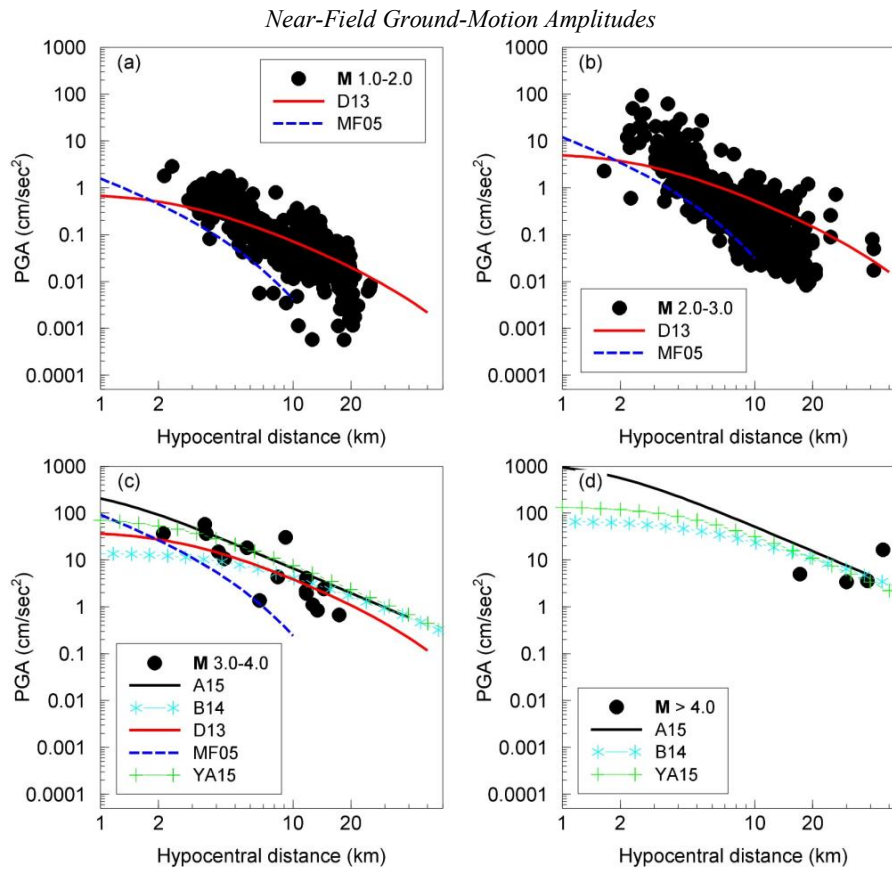


Fig. 4. Peak ground acceleration (PGA; RotD50), corrected for the B/C site condition ($V_{s30} = 760$ m/sec), is plotted versus hypocentral distance. Also plotted, are the attenuation models from McGarr and Fletcher (2005; MF05), Douglas et al., (2013; D13), Boore et al., (2014; B14), Atkinson (2015; A15), and Yenier and Atkinson (2015; YA15). Attenuation curves are for moment magnitude (M) 1.5, 2.5, 3.5, and 4.5.

Conclusions

In this paper, I looked at the ground-motion amplitudes from 241 potentially induced earthquakes in the Western Canada Sedimentary Basin. Moment magnitude (M) for the events without the reported M in the earthquake catalogue was calculated based on Atkinson et al. (2014) method using vertical component of response spectral acceleration at 1.0 and 3.3 Hz. Events fall within the M range of 1.0 to 4.6 with most events having focal depths of 3 to 4 km and recorded at hypocentral distances of < 50 km. Maximum horizontal motions (RotD100) from events with $M \geq 2.5$ are lower than the damage threshold at hypocentral distances > 5 km. At shorter distances, the observed PGA values may reach the damage threshold, suggesting that ground-motion amplitudes can become a high-frequency hazard. I used a diverse group of ground motion prediction equations (GMPEs) with the observed motions (RotD50) and their validity was investigated. For ground motions from M 1.0-3.0 events, the relation from Douglas et al. (2013) seems to match the ground-motion amplitudes although there is an underestimation for short hypocentral distances. The relation by McGarr and Fletcher (2005) underestimates PGA values for this magnitude range. For ground motions from events in the M range of 3 to 4, while the equation from McGarr and Fletcher (2005) clearly underestimates the PGA values, other GMPEs (Douglas et al., 2013, Boore et al., 2014, Atkinson, 2015, and Yenier and Atkinson, 2015) appear to match the data well. For the largest magnitude range ($M > 4.0$), it seems that Boore et al. (2014), Atkinson (2015), and Yenier and Atkinson (2015) estimate the ground-motion amplitudes relatively well.

Acknowledgements

This work was partially supported by Geoscience BC, BC Oil and Gas Research and Innovation Society, the Canadian Association of Petroleum Producers, and the ecoENERGY Innovation Initiative and the Environmental Geoscience Program of Natural Resources Canada.

References

- Atkinson, G. M., Greig, D. W., and Yenier, E. (2014). Estimation of moment magnitude (**M**) for small events (**M** < 4) on local networks, *Seismological Research Letters*, 85(5), pp. 1116-1124.
- Atkinson, G. M. (2015). Ground-motion prediction equation for small-to-moderate events at short hypocentral distances, with application to induced-seismicity hazards. *Bulletin of Seismological Society of America*, 105(2A), pp. 981-992.
- Atkinson, G. M. (2017). Strategies to prevent damage to critical infrastructure due to induced seismicity. *FACETS*, 2, pp. 374-394.
- Babaie Mahani, A. and Kao, H. (2018). Ground motion from M 1.5-3.8 induced earthquakes at hypocentral distance < 45 km in the Montney play of northeast British Columbia, Canada. *Seismological Research Letters*, 89(1), pp. 22-34.
- Babaie Mahani, A. and Kazemian, J. (2018). Strong ground motion from the November 12, 2017 **M** 7.3 Kermanshah earthquake in western Iran. *Journal of Seismology*, 22(6), pp. 1339-1358.
- Bommer, J. J. and Martinez-Pereira, A. (1999). The Effective Duration of Earthquake Strong Motion. *Journal of Earthquake Engineering*, 3, pp. 127-172.
- Boore, D. M. (2010). Orientation-independent, nongeometric-mean measures of seismic intensity from two horizontal components of motion. *Bulletin of Seismological Society of America*, 100(4), pp. 1830-1835.
- Boore, D. M., Stewart, J. P., Seyhan, E., and Atkinson, G. M. (2014). NGA-West2 equations for predicting PGA, PGV, and 5% damped PSA for shallow crustal earthquakes. *Earthquake Spectra*, 30, pp. 1057-1085.
- Douglas, J., Edwards, B., Convertito, V., Sharma, N., Tramelli, A., Kraaijpoel, D., Mena Cabrera, B., et al. (2013). Predicting ground motion from induced earthquakes in geothermal areas. *Bulletin of Seismological Society of America*, 103(3), pp. 1875-1897.
- Hassani, B. and Atkinson, G. M. (2016). Applicability of the site fundamental frequency as a Vs30 proxy for central and eastern north America. *Bulletin of Seismological Society of America*, 106(2), pp. 653-664.
- McGarr, A. and Fletcher, J. B. (2005). Development of ground-motion prediction equations relevant to shallow mining-induced seismicity in the Trail Mountain area, Emery County, Utah. *Bulletin of Seismological Society of America*, 95(1), pp. 31-47.
- Taylor, O-D S., Lester, A. P., Lee III, T. A., and McKenna, M. H. (2018). Can repetitive small magnitude-induced seismic events actually caused damage?. *Advances in Civil Engineering*, 2018, 5 pages.
- Worden, C. B., Gerstenberger, M. C., Rhoades, D. A., and Wald, D. J. (2012). Probabilistic relationships between ground-motion parameters and modified mercalli intensity in California. *Bulletin of Seismological Society of America*, 102(1), pp. 204-221.
- Yenier, E. and Atkinson, G. M. (2015). Regionally adjustable generic ground-motion prediction equation based on equivalent point-source simulations: application to central and eastern North America. *Bulletin of Seismological Society of America*, 105(4), pp. 1989-2009.



Banff 2018 International Induced Seismicity Workshop
October 24 – 27, 2018

Hydraulic Fracturing: A Regulatory Perspective for England

Anna L. Stork, School of Earth Sciences, University of Bristol, UK, anna.stork@bristol.ac.uk

Ian Davey, Environment Agency, England

Jim Grundy, Environment Agency, England

Regulation of the oil and gas industry in England is aimed at achieving the highest possible environmental standards. Hydraulic fracturing operators must demonstrate, to the satisfaction of the Environment Agency, their plan to monitor their operations to ensure that fractures remain within permitted formations and do not create potential pollutant pathways and hence risks to groundwater. The Agency currently consider seismic monitoring an appropriate method to achieve this objective and they are working with companies and universities to drive continual improvement in regulation and groundwater protection. This paper will outline the current regulations and their practical application in this nascent UK industry.

Introduction

The UK government currently believes that the development of shale gas exploration in the UK has the potential to provide the country with improved energy security accompanied by economic benefits. However, there is a significant level of concern in the population about the safety and environmental impact that the industry could have in the areas where development takes place. There is therefore regulation in place to assure all stakeholders that the necessary steps are followed to minimise risk and negative impacts. This includes the protection of groundwater, a significant area of regulation for the Environment Agency.

Environment Agency approach to regulation

The Environment Agency (EA) is one regulatory body of onshore oil and gas activities in England and it is the role of the Agency to carry out government policy to protect groundwater during these activities. The other regulators are the Oil and Gas Authority (OGA), who regulate the induced seismicity traffic light scheme (TLS), and the Health and Safety Executive (HSE), responsible for health and safety onsite. Unconventional hydraulic fracturing operations are covered by different pieces of legislation, including the Environmental Permitting (England and Wales) Regulations. These require a permit for discharge of substances into ground, where these could impact on groundwater, and for waste management (Environment Agency, 2016). Under these regulations entry into groundwater of defined ‘hazardous substances’ and pollution by ‘non-hazardous pollutants’ must be prevented. In addition, any hydraulic fracturing fluid left in the ground is considered a waste product and, therefore, to obtain a permit, operators must set out how they will monitor the hydraulic fracturing fluid, where it goes and how they will report the information to the EA. The induced fractures and injected fluids must remain

within the permitted boundary, a permitted volume of operation within a geological formation agreed by the regulators.

Several options are available to monitor fluid flow, including fluid injection rate and pressure monitoring, and fracture modelling is an important tool to predict the response of the reservoir. However, the Agency currently consider microseismic monitoring the most suitable monitoring approach to assess the extent of hydraulic fracturing fluid during operations due the ability of the technology to provide an estimate of fracture height and length (e.g., Fisher and Warpinski, 2012).

Approved microseismic monitoring approaches

The information as to how the microseismic monitoring will be carried out is provided to the EA in the form of a Hydraulic Fracture Plan (HFP) and, to date, two plans have been approved. The first, provided by Third Energy Ltd for the Kirby Misperton site in North Yorkshire, included plans to deploy a geophone array consisting of 10 3-component instruments in an existing borehole and at a depth of approximately 1200 m and approximately 900 m above the shallowest planned hydraulic fracturing stage (Figure 1a). The geophones would be positioned in a suspended deviated vertical well, on the same well pad as the vertical treatment well. It was estimated that the magnitude (M) detection threshold at the top of the permitted zone was M-2.6 and M-1.9 at the bottom of the permitted zone. Estimated location errors were 10 m in depth and 30 m laterally at the shallowest stimulation interval and 30 m in depth and 100 m laterally at the deepest stimulation interval. It was planned to conduct continuous recording with the array during operations and provide an initial analysis of results (location and magnitude) within 5 minutes. If results indicated that fracturing was propagating in a way that it may extend outside the permitted boundary then the stimulation would be paused to assess the situation. The final estimated fracture dimensions would be reported to the EA after each stage of stimulation. Third Energy's HFP is available from EA website (consult.environment-agency.gov.uk).

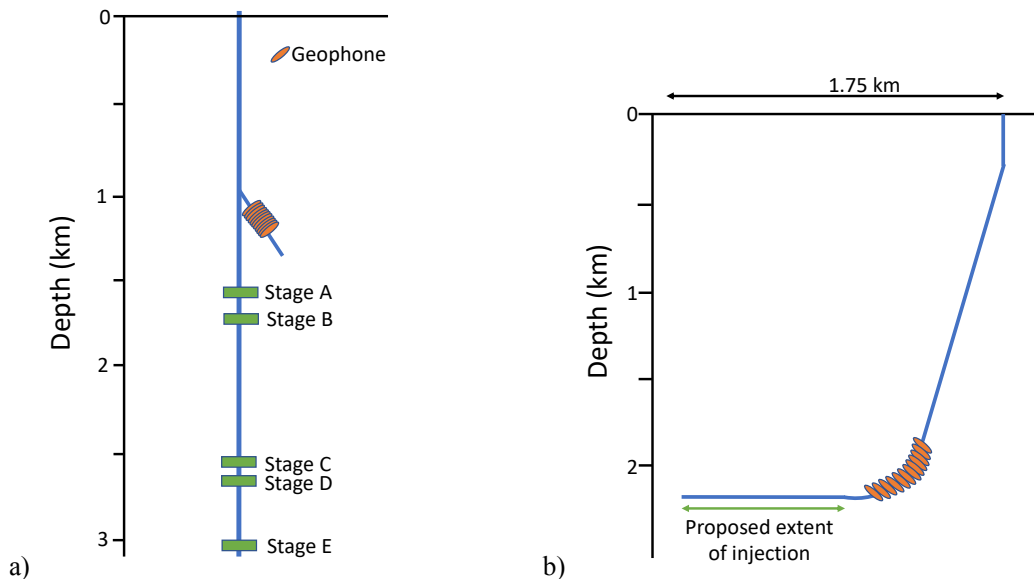


Fig. 1. a) Schematic of Third Energy's proposed microseismic monitoring set-up. The geophones are in a suspended well on the same well pad as the injection well. b) Schematic of Cuadrilla Resources' proposed microseismic monitoring set-up. The geophones are in an observation well adjacent to the injection well.

The other HFP to be approved was submitted by Cuadrilla Resources Ltd for the Preston New Road site in Lancashire. The approach taken to understand fracture growth and extent with microseismic monitoring is to

deploy 12 slim 3-component 15 Hz geophones. These will be positioned at the heel of an observation well, adjacent to the injection well. The estimated limit of detectability at the toe of the injection well is local magnitude, M_L -1.8 with estimated errors in location of 20 m in x, y and z. If the microseismic event locations indicate a flow pathway close to the edge of the permitted boundary pumping will be reduced or suspended and the HFP modified to prevent a breach of the permitted boundary. The microseismic monitoring data will be processed in real-time during operations. Cuadrilla Resources' HFP is available from EA website (consult.environment-agency.gov.uk).

Evolution of regulatory approach

The Agency recognises that there are limits to the technologies available to monitor industrial activities. In particular, microseismic monitoring does not provide information on any aseismic fluid flow and the occurrence of a microseismic event does not necessarily indicate the presence of hydraulic fracturing fluids. One possibility to help determine the extent of frac fluids, and distinguish “wet” from “dry” fracks, is to assume linear pore pressure diffusion rates (e.g., Shapiro and Dinske, 2009), although the validity of this assumption cannot normally be verified. The EA also appreciate that technology is constantly evolving to help solve such difficulties and are therefore actively engaged in discussion and collaborations with universities and overseas regulators (e.g., the Alberta Energy Regulator). This will enable them to maintain an appropriate level of regulation by taking account of the currently available techniques and their capabilities and limitations.

Conclusions

The Environment Agency England currently consider microseismic monitoring the most appropriate available method to assess fracture and hence hydraulic fracturing fluid extent during operations. The hydraulic fracturing industry is nascent in the UK and the Environment Agency is working with companies and universities to drive continual improvement in regulation and groundwater protection. The Agency is particularly interested in understanding advancements in fracture monitoring and progress made in the capabilities of microseismic monitoring to ensure regulation takes account of good practice development.

Acknowledgements

The work by ALS was supported by the Natural Environment Research Council (grant numbers NE/R006709/1 and NE/R014531/1).

References

- Environment Agency, England 2016. Onshore oil and Gas Sector Guidance, v.1 <https://www.gov.uk/government/publications/onshore-oil-and-gas-exploration-and-extraction-environmental-permits> (last accessed Sept. 2018).
- Fisher, K. and N. Warpinski (2012). Hydraulic-fracture height growth: Real data, SPE Production & Operations, 27(1), SPE-145949-PA, doi:10.2118/145949-PA.
- Shapiro, S. A., and C. Dinske (2009), Scaling of seismicity induced by nonlinear fluid-rock interaction, J. Geophys. Res., 114, B09307, doi:10.1029/2008JB006145.



Banff 2018 International Induced Seismicity Workshop
October 24 – 27, 2018

Using Beamforming to Maximise the Detection Capability of Small, Sparse Seismometer Arrays

James P. Verdon, School of Earth Sciences, University of Bristol, James.Verdon@bristol.ac.uk

Michael Kendall, School of Earth Sciences, University of Bristol, gljmk@bristol.ac.uk

Stephen P. Hicks, Ocean and Earth Science, University of Southampton, s.hicks@soton.ac.uk

Philip Hill, Guralp Systems Ltd., Aldermaston, UK, phill@guralp.com

Nadine Igonin, Department of Geosciences, University of Calgary, naigonin@ucalgary.ca

As concerns about induced seismicity continue, we are increasingly seeing the deployment of site-specific monitoring networks of surface seismometers, often with a relatively large number of stations ($N = 10 - 20$ or more). In this paper we develop and demonstrate a beamforming (delay-and-stack) method that, in comparison to conventional event detection algorithms, produces (i) improved detection thresholds, and (ii) allows events to be detected without the need for manual picking. We demonstrate this approach using two case studies of hydraulic fracturing-induced seismicity. In the first study, in Oklahoma, the site had been monitored using 17 surface seismometers. In the second, in Alberta, the site had been monitored with 68 shallow borehole geophones. In both cases, the beamforming approach produced a significant increase in the number of detected events compared to conventional event-picking based analysis.

Introduction

As operating companies and regulators have recognised the significance of induced seismicity, we have seen an increase in the deployment of site-specific local monitoring arrays. Where such arrays have a relatively large number of stations ($N = 10 - 20$ or more), novel methods of event detection and location become possible. Rather than relying on trigger detection at individual stations using forms of time-series analysis (spikes in STA/LTA ratios for example), methods that base event detection on combined signals across a large- N array have shown significant potential for improved event detection.

In this paper we outline such an approach, using beamforming (delay-and-stack) methods to boost the signal from small magnitude events. This allows us to detect and locate events that, because of their low signal-to-noise ratio (SNR), could not be detected using conventional single-station methods. The beamforming method also determines the event hypocentre without the need for manual phase picking, which both introduces a degree of subjectivity to the results, depending on the skill of the processor, and can be time-consuming in cases where a large number of events are recorded. We demonstrate this approach using two case studies (Verdon et al., 2017; Eaton et al., 2018) where local, site-specific arrays had been deployed to monitor induced seismicity associated with hydraulic fracturing.

Method

Consider a set of waveforms detected by an array, which may contain a low-magnitude seismic event. We perform a search over candidate event locations within a defined region of interest. For a candidate location \mathbf{x} , we begin by rotating the observed waveforms into a $[P, S_H, S_V]$ coordinate system, with the assumption that, due to ray-bending effects in the subsurface, the P component is vertical. For each component we compute a running short-time/long-time average (STA/LTA) using the Allen (1978) method, where for each trace y at time sample i :

$$C(i) = y(i)^2 + 3(y(i) - y(i-1))^2 ;$$

$$STA(i) = \frac{\sum_{j=i}^{i+n_s-1} C(j)}{n_s} ; LTA(i) = \frac{\sum_{j=i-n_l}^{i-1} C(j)}{n_l} ; R(i) = STA(i)/LTA(i)$$

The STA/LTA time series for each trace is time-shifted based on the modelled P or S phase differential travel time from \mathbf{x} to station k :

$$dt_P(\mathbf{x}, k) = t_P(\mathbf{x}, k) - \min(t_P(\mathbf{x}, :)) ; dt_S(\mathbf{x}, k) = t_S(\mathbf{x}, k) - \min(t_S(\mathbf{x}, :)).$$

The aligned traces are then summed over the n stations to create a stack:

$$\Psi_P(\mathbf{x}, i) = \frac{[\sum_{k=1}^n R_P^k(i - \frac{dt_P(\mathbf{x}, k)}{\delta})]}{n} ; \Psi_{S_H}(\mathbf{x}, i) = \frac{[\sum_{k=1}^n R_{S_H}^k(i - \frac{dt_{S_H}(\mathbf{x}, k)}{\delta})]}{n} ; \Psi_{S_V}(\mathbf{x}, i) = \frac{[\sum_{k=1}^n R_{S_V}^k(i - \frac{dt_{S_V}(\mathbf{x}, k)}{\delta})]}{n} ;$$

where δ is the time series sampling rate. The overall stack is determined from the product of the P , S_H , and S_V stacks:

$$S(\mathbf{x}, i) = \Psi_P(\mathbf{x}, i)\Psi_{S_H}(\mathbf{x}, i)\Psi_{S_V}(\mathbf{x}, i).$$

The resulting stack function is a 4-dimensional function of both spatial position and time. However, the function can be simplified to take the maximum value at each spatial point within a given time window i to $i + \tau$, reducing the results to a 3D data cube (e.g., Chambers et al., 2010):

$$S'(\mathbf{x}) = \max(S(\mathbf{x}, \{i, \dots, i + \tau\})).$$

We note that the stack power as a function of candidate position tends not to be particularly smooth: local maxima are common. Therefore directional search algorithms are not appropriate, as they tend to become trapped in these local maxima. Instead, global search algorithms are required. Grid searches are commonly used with beamforming and stacking type event detection algorithms (e.g., Chambers et al., 2010). However, a grid-search over 3 spatial dimensions can be hugely expensive from a computational point of view, making the use of such methods in real-time a challenging proposition. In this paper we find that the Neighbourhood Algorithm described by Sambridge (1999a) provides an adequate search of the parameter space while significantly reducing computation time.

Case Study #1: Oklahoma

Our first case study is from a hydraulic fracturing treatment in Oklahoma. The site was monitored using an array of 17 surface seismometers (Verdon et al., 2017). Monitoring of stimulation in 2 horizontal wells, at a depth of c. 3.8 km, took place over 8 days. Initially, event detection was performed using a standard single-trace STA/LTA-based triggering algorithm that is commonly used in seismology (Lomax et al., 2012). Events were identified when triggers occurred simultaneously (within 3 seconds on at least four stations. For these events, P- and S-wave arrivals were manually re-picked, and the phase arrival times were inverted for event locations. A total of 17 events were detected in this manner (Fig. 1a). The events are clustered around the treatment wells and range in magnitude from $0 < M_W < 1$.

For the beamforming approach, the data were divided into 30-second intervals, with 5 seconds of overlap. Within each interval we perform a search for candidate event locations using the method described above. Based on both synthetic modelling and analysis of the initial results, we set a threshold for event detection of $S'(\mathbf{x}) > 15$. The

event hypocentre is taken as the point where $S'(\mathbf{x})$ is maximised. A total of 155 events were detected (Figure 1b), a significant increase on the 17 events detected using the conventional triggering algorithm. We note that the event hypocentres migrate with time from the toes to the heels of the wells, as expected given typical HF programs, indicating that the detected events are real and are robustly located.

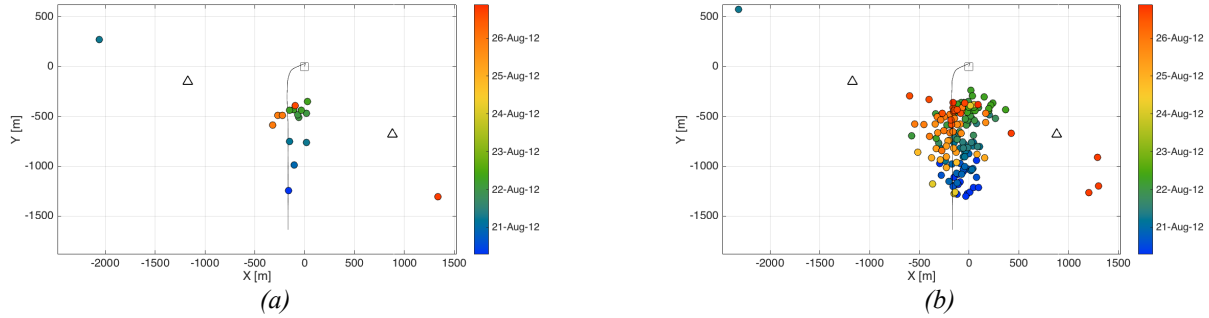


Fig. 1. Map views of event locations from the Oklahoma case study. In (a) we show the events detected by conventional picking analysis, and in (b) we show the events detected by the beamforming approach.

Fig. 2 shows the waveforms from two events, one of which had a high SNR and was detected by both methods, and one of which had a low SNR and was only detected by the beamforming method. Fig. 2 also shows slices through $S'(\mathbf{x})$ for these two events. While the weak event is barely discernible on the raw traces, the stacking function shows a clear and well defined peak, which allows the event to be robustly detected.

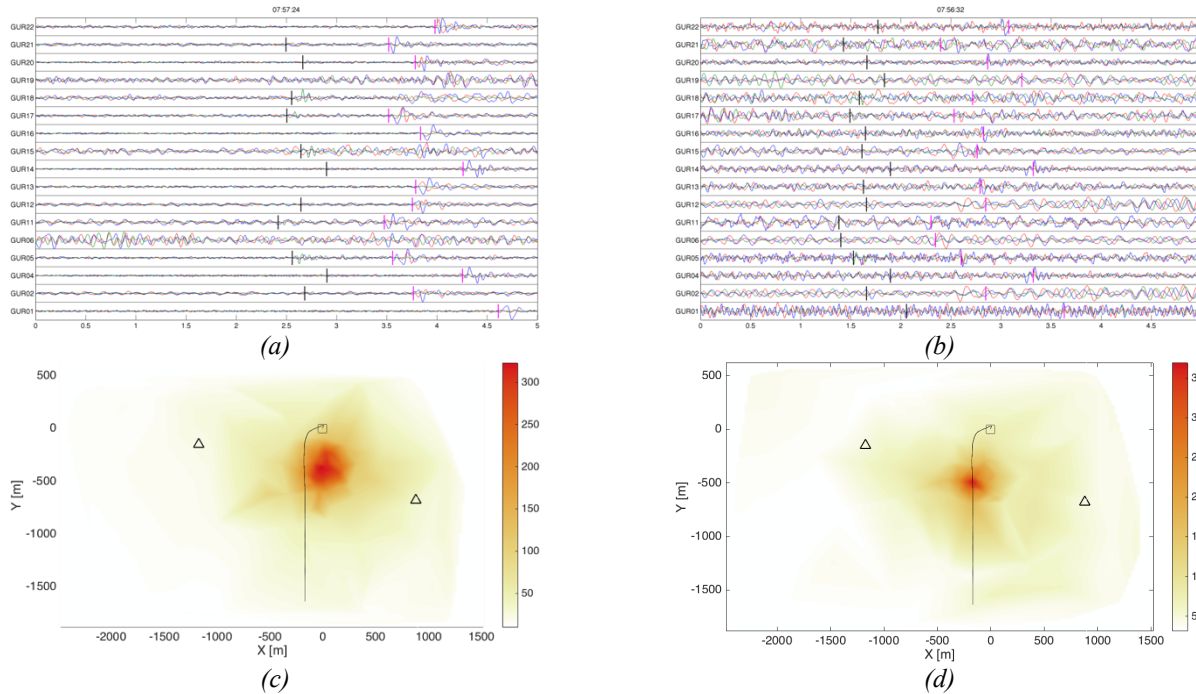


Fig. 2. Waveforms from two events with (a) high SNR and (b) low SNR. The high SNR event was detected by the conventional picking algorithm, but the low SNR event was not. In (c) and (d) we show map views of $S'(\mathbf{x})$ for the high and low SNR events: in both cases a clear peak in $S'(\mathbf{x})$ marks the event location.

Case Study #2: ToC2ME, Fox Creek, Alberta

Our second case study comes from the Tony Creek Dual Microseismic Experiment (ToC2ME), where 68 shallow borehole stations were deployed to monitor hydraulic fracturing in the Duvernay Shale, near Fox Creek, Alberta (Eaton et al., 2018). Initial event detection was performed using an amplitude-based trigger, which generated a population of 15 “master” events that were used in a matched-filter algorithm to search for candidate events. A total of 25,146 candidate events were thereby produced. These events were then located using a relative location

method (Eaton et al., 2018) to produce the final event catalogue. However, limited SNR meant that only 4,083 events could be accurately located using this method.

We therefore used the beamforming approach to locate the remaining 21,063 low-magnitude events, as well as to relocate the high SNR 4,083 events to evaluate the quality of the results. As per the previous study (Verdon et al., 2017), we used $S'(\mathbf{x}) > 15$ as our QC criteria. A total of 18,472 events met this threshold, representing a significant increase on the number of events that could be manually located. As well as the increase in the number of events, this approach obviated the need for time-consuming manual picking on catalogues of thousands of events.

Our results are plotted in Fig. 3, comparing the events located by the relative location method with the events located by the beamforming algorithm. We note the significant improvement in event detection, which serves to outline in much more detail the features in the reservoir that have been reactivated during hydraulic fracturing. This allows us to make improved interpretations of the processes that occur when seismicity is induced during HF.

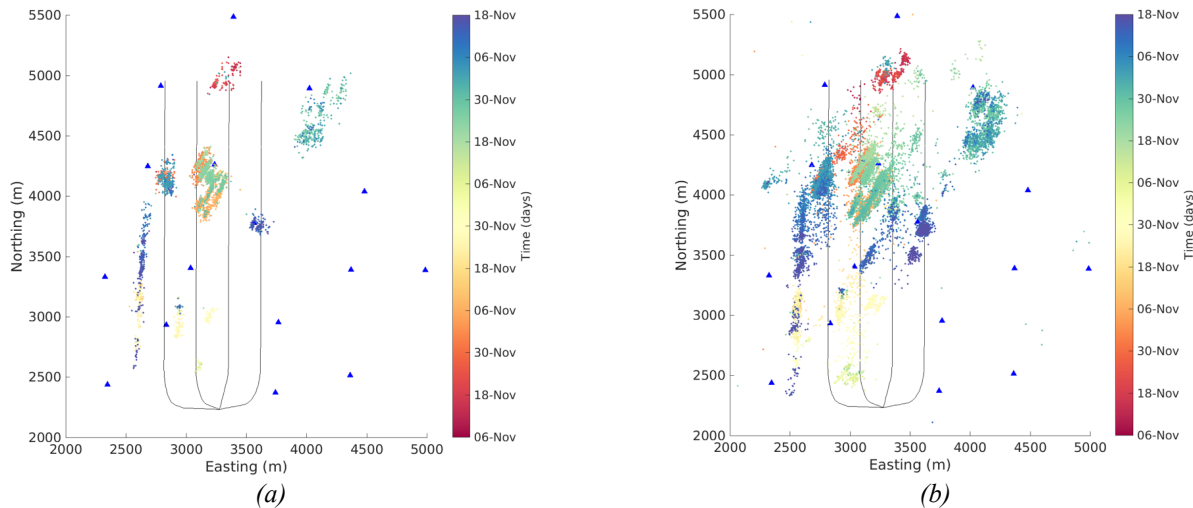


Fig. 3. Map views comparing the ToC2ME events that were located using (a) relative location method and (b) using the beamforming method. The improvement in event detection provided by the beamforming method reveals structures that cannot be seen using the relative location method.

Acknowledgements

The development of the beamforming algorithm was funded by Gralp Systems Ltd.. We would like to thank the operators of the Oklahoma site, and of the ToC2ME program, for providing the field data used to generate these results.

References

- Allen R.V., 1978. Automatic earthquake recognition and timing from single traces: *Bulletin of the Seismological Society of America* 68, 1521-1532.
- Chambers K., J-M. Kendall, S. Brandsberg-Dahl, J. Rueda, 2010. Testing the ability of surface arrays to monitor microseismic activity. *Geophysical Prospecting* 58, 821-830.
- Eaton D.W., N. Igonin, A. Poulin, R. Weir, H. Zhang, S. Pellegrino, G. Rodriguez, 2018. Induced seismicity characterisation during hydraulic-fracture monitoring with a shallow-wellbore geophone array and broadband sensors. *Seismological Research Letters*, *in press*.
- Lomax A., C. Satriano, M. Vassallo, 2012. Automatic picker developments and optimization: FilterPicker – a robust, broadband picker for real-time seismic monitoring and earthquake early warning. *Seismological Research Letters* 83, 531-540.
- Verdon J.P., J-M. Kendall, S.P. Hicks, P. Hill, 2017. Using beamforming to maximise the detection capability of seismometer arrays deployed to monitor oilfield activities. *Geophysical Prospecting* 65, 1582-1596.